Supplementary Information

T7 RNA polymerase non-specifically transcribes and induces disassembly of DNA nanostructures

Samuel W. Schaffter[a], Leopold Green[b], Joanna Schneider[a], Hari K.K. Subramanian[b], Rebecca Schulman,[a, c] and Elisa Franco[b]

[a]Department of Chemical and Biomolecular Engineering – Johns Hopkins University, [b]Department of Mechanical Engineering – University of California - Riverside, [c]Department of Computer Science – Johns Hopkins University

Table of Contents

1. Designs and sequences of nanotube variants and other DNA

1.1 DNA tile designs and sequences

var1_7

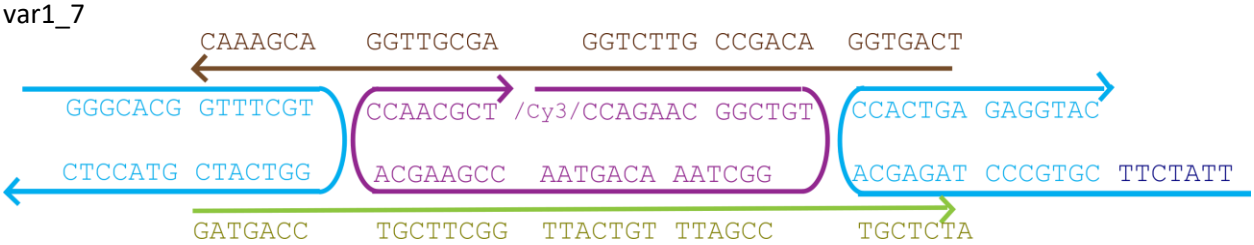

Strand name	Sequence
var1_7 strand 1	5′ TCAGTGGACAGCCGTTCTGGAGCGTTGGACGAAAC
var1_7 strand 2	5′ TTATCTTCGTGCCCTAGAGCACCACTGAGAGGTAC
var1 strand 3	/5Cy3/CCAGAACGGCTGTGGCTAAACAGTAACCGAAGCACCAACGCT
var1_7 strand 4	5′ GGGCACGGTTTCGTGGTCATCGTACCTC
var1_7 strand 5	5′ GATGACCTGCTTCGGTTACTGTTTAGCCTGCTCTA

var2_7

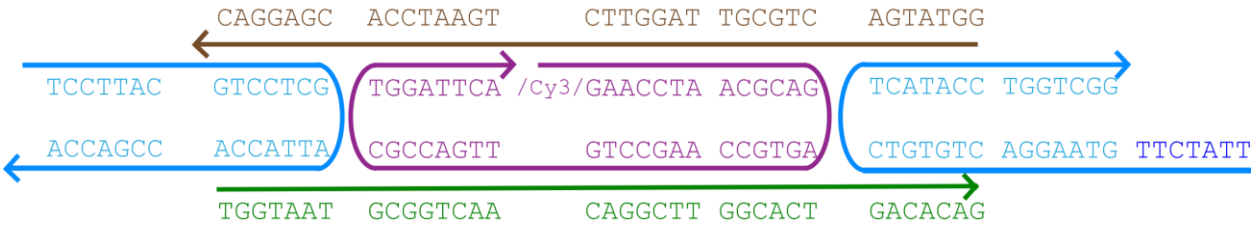

Strand name	Sequence
var2_7 strand 1	5′ GGTATGACTGCGTTAGGTTCTGAATCCACGAGGAC
var2_7 strand 2	5′ TTATCTTGTAAGGACTGTGTCTCATACCTGGTCGG
var2 strand 3	T/iCy3/GAACCTAACGCAGAGTGCCAAGCCTGTTGACCGCTGGATTCA
var2_7 strand 4	TCCTTACGTCCTCGATTACCACCGACCA
var2_7 strand 5	5′ TGGTAATGCGGTCAACAGGCTTGGCACTGACACAG

var3_7

Strand name	Sequence
var1_7 strand 1	5′ TCAGTGGACAGCCGTTCTGGAGCGTTGGACGAAAC
var3_7 strand 2	5′ TGGTATTTGTCTGGTAGAGCACCACTGAGAGGTAC
var1 strand 3	/5Cy3/CCAGAACGGCTGTGGCTAAACAGTAACCGAAGCACCAACGCT
var3_7 strand 4	5′ CCAGACAGTTTCGTGGTCATCGTACCTC
var1_7 strand 5	5′ GATGACCTGCTTCGGTTACTGTTTAGCCTGCTCTA

var4_7

Strand name	Sequence
var1_7 strand 1	5′ TCAGTGGACAGCCGTTCTGGAGCGTTGGACGAAAC
var4_7 strand 2	5′ TGGTATTCGTCGGGTAGAGCACCACTGAGAGGTAC
var1 strand 3	/5Cy3/CCAGAACGGCTGTGGCTAAACAGTAACCGAAGCACCAACGCT
var4_7 strand 4	5′ CCCGACGGTTTCGTGGTCATCGTACCTC
var1_7 strand 5	5′ GATGACCTGCTTCGGTTACTGTTTAGCCTGCTCTA

var5_7

Strand name	Sequence
var1_7 strand 1	5′ TCAGTGGACAGCCGTTCTGGAGCGTTGGACGAAAC
var5_7 strand 2	5′ TGGTATTTGTCTGGTAGAGCACCACTGAGGCCTGC
var1 strand 3	/5Cy3/CCAGAACGGCTGTGGCTAAACAGTAACCGAAGCACCAACGCT
var5_7 strand 4	5′ CCAGACAGTTTCGTGGTCATCGCAGGCC
var1_7 strand 5	5′ GATGACCTGCTTCGGTTACTGTTTAGCCTGCTCTA

var6_7

Strand name	Sequence
var1_7 strand 1	5′ TCAGTGGACAGCCGTTCTGGAGCGTTGGACGAAAC
var6_7 strand 2	5′ TGGTATTCGTCGGGTAGAGCACCACTGAGAGGCGC
var1 strand 3	/5Cy3/CCAGAACGGCTGTGGCTAAACAGTAACCGAAGCACCAACGCT
var6_7 strand 4	5′ CCCGACGGTTTCGTGGTCATCGCGCCTC
var1_7 strand 5	5′ GATGACCTGCTTCGGTTACTGTTTAGCCTGCTCTA

var1_7-1

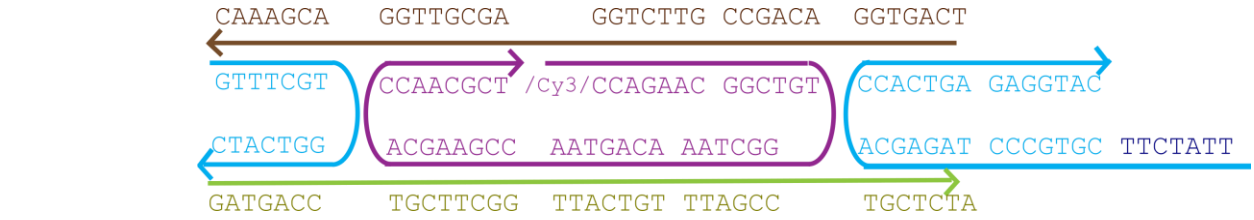

Strand name	Sequence
var1_7 strand 1	5′ TCAGTGGACAGCCGTTCTGGAGCGTTGGACGAAAC
var1_7 strand 2	5′ TTATCTTCGTGCCCTAGAGCACCACTGAGAGGTAC
var1 strand 3	/5Cy3/CCAGAACGGCTGTGGCTAAACAGTAACCGAAGCACCAACGCT
var1_7-1 strand 4	5′ GTTTCGTGGTCATC
var1_7 strand 5	5′ GATGACCTGCTTCGGTTACTGTTTAGCCTGCTCTA

var1_7-2

Strand name	Sequence
var1_7 strand 1	5′ TCAGTGGACAGCCGTTCTGGAGCGTTGGACGAAAC
Ortho. var1_7 strand 2	5′ AATTTAACGTGCCCTAGAGCACCACTGAGAGGTAC
var1 strand 3	/5Cy3/CCAGAACGGCTGTGGCTAAACAGTAACCGAAGCACCAACGCT
var1_7 strand 4	5′ GGGCACGGTTTCGTGGTCATCGTACCTC
var1_7 strand 5	5′ GATGACCTGCTTCGGTTACTGTTTAGCCTGCTCTA

var1_7-3

Strand name	Sequence
var1_7 strand 1	5′ TCAGTGGACAGCCGTTCTGGAGCGTTGGACGAAAC
var1_7-3 strand 2F	/56FAM/GATAGAACGTGCCCTAGAGCACCACTGAGAGGTAC
var1 strand 3	/5Cy3/CCAGAACGGCTGTGGCTAAACAGTAACCGAAGCACCAACGCT
var1_7 strand 4	5′ GGGCACGGTTTCGTGGTCATCGTACCTC
var1_7 strand 5	5′ GATGACCTGCTTCGGTTACTGTTTAGCCTGCTCTA

var1_6

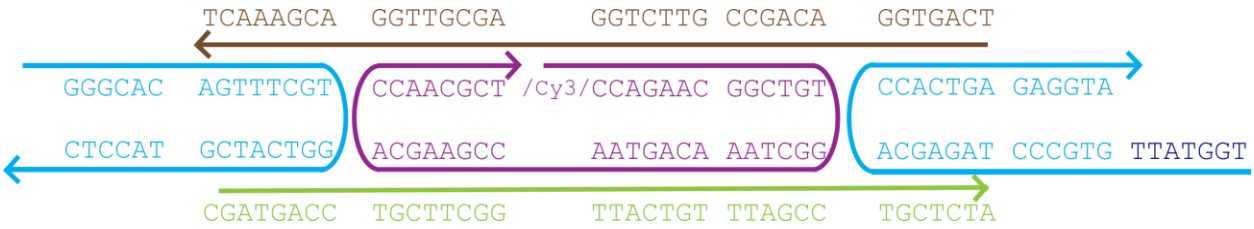

Strand name	Sequence
var1_6 strand 1	5′ TCAGTGGACAGCCGTTCTGGAGCGTTGGACGAAACT
var1_6 strand 2	5′ TTATCTTGTGCCCTAGAGCACCACTGAGAGGTA
var1 strand 3	/5Cy3/CCAGAACGGCTGTGGCTAAACAGTAACCGAAGCACCAACGCT
var1_6 strand 4	5′ GGGCACAGTTTCGTGGTCATCGTACCTC
var1_6 strand 5	5′ CGATGACCTGCTTCGGTTACTGTTTAGCCTGCTCTA

var3_6

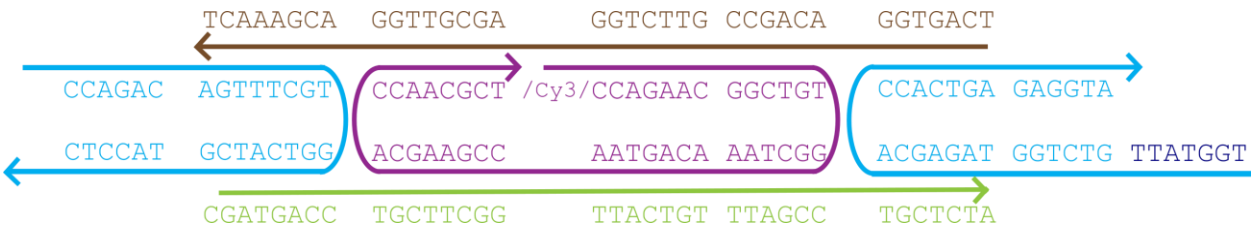

Strand name	Sequence
var1_6 strand 1	5′ TCAGTGGACAGCCGTTCTGGAGCGTTGGACGAAACT
var3_6 strand 2	5′ TGGTATTGTCTGGTAGAGCACCACTGAGAGGTA
var1 strand 3	/5Cy3/CCAGAACGGCTGTGGCTAAACAGTAACCGAAGCACCAACGCT
var3_6 strand 4	5′ CCAGACAGTTTCGTGGTCATCGTACCTC
var1_6 strand 5	5′ CGATGACCTGCTTCGGTTACTGTTTAGCCTGCTCTA

var1_8

Strand name	Sequence
var1_8 strand 1	5′ AGTGGACAGCCGTTCTGGAGCGTTGGACGAAACT
var1_8 strand 2	5′ TGTAATATCGTGCCCGAGCACCACTGAGAGGTA
var1 strand 3	/5Cy3/CCAGAACGGCTGTGGCTAAACAGTAACCGAAGCACCAACGCT
var1_8 strand 4	5′ GGGCACGAAGTTTCGTGGTCATCGTACCTCTC
var1_8 strand 5	5′ CGATGACCTGCTTCGGTTACTGTTTAGCCTGCTC

var3_8

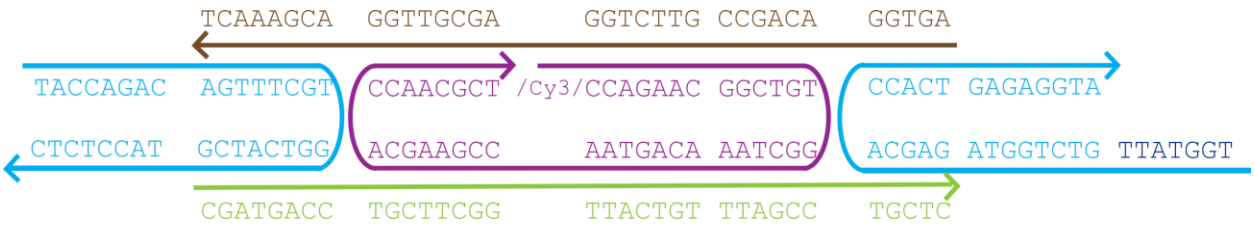

Strand name	Sequence
var1_8 strand 1	5′ AGTGGACAGCCGTTCTGGAGCGTTGGACGAAACT
var3_8 strand 2	5′ TGGTATTGTCTGGTAGAGCACCACTGAGAGGTA
var1 strand 3	/5Cy3/CCAGAACGGCTGTGGCTAAACAGTAACCGAAGCACCAACGCT
var3_8 strand 4	5′ TACCAGACAGTTTCGTGGTCATCGTACCTCTC
var1_8 strand 5	5′ CGATGACCTGCTTCGGTTACTGTTTAGCCTGCTC

var1_7 7bp hairpin stem

Strand name	Sequence
var1_7 strand 1	5′ TCAGTGGACAGCCGTTCTGGAGCGTTGGACGAAAC
var1_7 7bpHP strand 2	5′ AAGATAATTTTTTATCTTCGTGCCCTAGAGCACCACTGAGAGGTAC
var1 strand 3	/5Cy3/CCAGAACGGCTGTGGCTAAACAGTAACCGAAGCACCAACGCT
var1_7 strand 4	5′ GGGCACGGTTTCGTGGTCATCGTACCTC
var1_7 strand 5	5′ GATGACCTGCTTCGGTTACTGTTTAGCCTGCTCTA

var1_7 5bp hairpin stem

Strand name	Sequence
var1_7 strand 1	5′ TCAGTGGACAGCCGTTCTGGAGCGTTGGACGAAAC
var1_7 5bpHP strand 2	5′ GATAATTTTTTATCTTCGTGCCCTAGAGCACCACTGAGAGGTAC
var1 strand 3	/5Cy3/CCAGAACGGCTGTGGCTAAACAGTAACCGAAGCACCAACGCT
var1_7 strand 4	5′ GGGCACGGTTTCGTGGTCATCGTACCTC
var1_7 strand 5	5′ GATGACCTGCTTCGGTTACTGTTTAGCCTGCTCTA

var3_7 7bp hairpin stem

Strand name	Sequence
var1_7 strand 1	5′ TCAGTGGACAGCCGTTCTGGAGCGTTGGACGAAAC
var3_7 7bpHP strand 2	5′ AATACCATTTTTGGTATTTGTCTGGTAGAGCACCACTGAGAGGTAC
var1 strand 3	/5Cy3/CCAGAACGGCTGTGGCTAAACAGTAACCGAAGCACCAACGCT
var3_7 strand 4	5′ CCAGACAGTTTCGTGGTCATCGTACCTC
var1_7 strand 5	5′ GATGACCTGCTTCGGTTACTGTTTAGCCTGCTCTA

var3_7 5bp hairpin stem

Strand name	Sequence
var1_7 strand 1	5′ TCAGTGGACAGCCGTTCTGGAGCGTTGGACGAAAC
var3_7 5bpHP strand 2	5′ TACCATTTTTGGTATTTGTCTGGTAGAGCACCACTGAGAGGTAC
var1 strand 3	/5Cy3/CCAGAACGGCTGTGGCTAAACAGTAACCGAAGCACCAACGCT
var3_7 strand 4	5′ CCAGACAGTTTCGTGGTCATCGTACCTC
var1_7 strand 5	5′ GATGACCTGCTTCGGTTACTGTTTAGCCTGCTCTA

1.2 Fluorescent RNA transcript probes

Cy3 strand 3 var1_7 probe

```
var1 strand 3          /5Cy3/CCAGAACGGCTGTGGCTAAACAGTAACCGAAGCACCAACGCT
```

Orthogonal probe

```
Orthogonal probe       /5Cy3/TCTACGGAAATGTGGCAGAATCAATCATAAGACACCAGTCGG
```

var2_7 probe

```
var2 strand 3          T/iCy3/GAACCTAACGCAGAGTGCCAAGCCTGTTGACCGCTGGATTCA
```

1.3 Overhang complementary strand for confirmation of FAM fluorescence change system

```
Overhang complementary strand   5' GGGCACGTTCTATCTATTCT
```

1.4 T7 RNAP promoter containing duplex

```
Non-template strand   5' AAGCAAGGGTAAGATGGAATGATAATACGACTCACTATAGGGAA
Template strand       5' TTCCCTATAGTGAGTCGTATTATCATTCCATCTTACCCTTGCTT
```

2 PCR protocols

Nanotube annealing protocol

Step	Temperature	Rate	Time	Repeat	Total time
1	90C	-	5 min	1	5 min
2	90C	-0.1 °C/cycle	6 sec	99	10 min
3	80C	-0.1 °C/ cycle	6 sec	99	10 min
4	70C	-0.1 °C/ cycle	6 sec	99	10 min
5	60C	-0.1 °C/ cycle	1 min	99	100 min
6	50C	-0.1 °C/ cycle	1 min	99	100 min
7	40C	-0.1 °C/ cycle	1 min	99	100 min
8	30C	-0.1 °C/ cycle	6 sec	99	10 min
9	20C	-	60 min	1	60 min
10	25C	-	Hold	1	15 – 18 hr

This protocol was used to anneal all DNA nanotubes tested throughout the study.

Characterization of RNA transcript

Step	Temperature	Rate	Time	Repeat	Total time
1	37C	-	20 hr	1	20 hr
2	65C	-	30 min	1	30 min
3	37C	-	2 hr	1	2 hr
3a	37C	-	4.5hr	1	4.5 hr

Detecting tile-specific sequences in RNA with fluorescent DNA probes

Step	Temperature	Rate	Time	Repeat	Total time
1	37C	-	20 hr	1	20 hr
2	65C	-	30 min	1	30 min
3	37C	-	24 hr	1	24 hr
5	75C	-	30 min	1	30 min
7	90C	-	5 min	1	5 min
8	90C	-0.1 °C/cycle	6 sec	99	10 min
9	80C	-0.1 °C/cycle	6 sec	99	10 min
10	70C	-0.1 °C/cycle	6 sec	99	10 min
11	60C	-0.1 °C/cycle	6 sec	99	10 min
12	50C	-0.1 °C/cycle	6 sec	99	10 min
13	40C	-0.1 °C/cycle	6 sec	99	10 min
14	30C	-0.1 °C/cycle	6 sec	49	10 min
15	25C	-	Hold	1	-

RNA solution preparation

Step	Temperature	Rate	Time	Repeat	Total time
1	37C	-	20 hr	1	20 hr
2	65C	-	30 min	1	30 min
3	37C	-	24 hr	1	24 hr
5	75C	-	30 min	1	30 min
7	37C	-	Hold	1	-

3 A single-stranded overhang promotes nanotube growth in transcription buffer

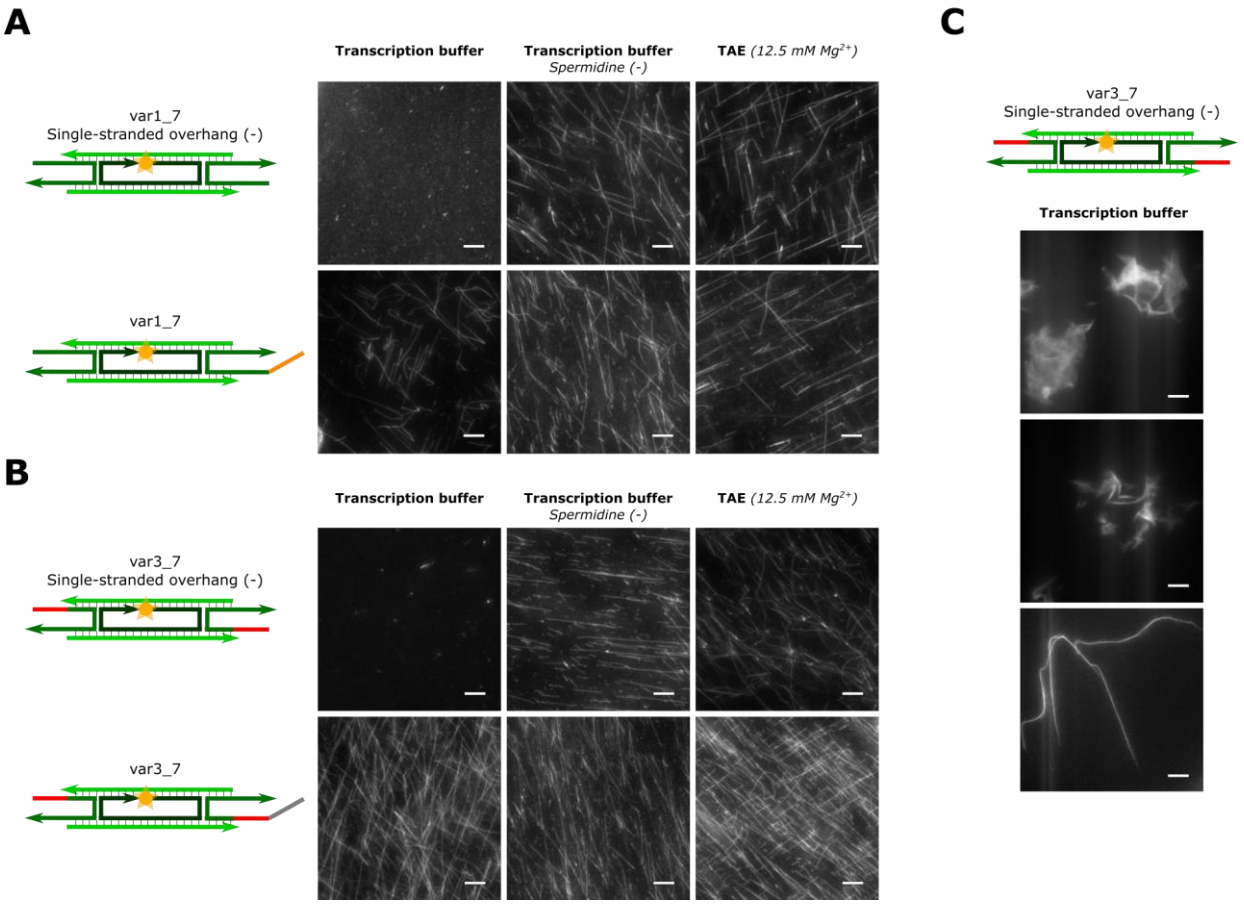

Supplementary Figure S1: DNA tiles without a single-stranded overhang on strand 2 do not assemble into nanotubes in the presence of spermidine. **A)** and **B)** Fluorescence micrographs of **A)** var1_7 tile variants or **B)** var3_7 tile variants annealed in NEB RNAPol transcription buffer, RNAPol transcription buffer without spermidine, or Tris-Acetate-EDTA (TAE) buffer containing 12.5 mM Mg^{2+} with (bottom panels) or without (top panels) a single-stranded overhang domain on strand 2 of the tiles. Nanotubes were annealed as described in *Measurement of nanotube stability* in the Methods of the main text. **C)** Additional fluorescence micrographs of the var3_7 tile variants without a single-stranded overhang annealed in NEB RNAPol transcription buffer. Tiles without the single-stranded overhang domain appear to cluster or aggregate when spermidine is present. Scale bars: 10 µm. Fluorescence micrographs were taken after the samples were diluted to a tile concentration of 250 nM.

The ability of DNA nanotubes without single-stranded overhangs to self-assemble in TAE Mg^{2+} but not in transcription buffer (Supplementary Figure S1) suggested that self-assembly was impeded by components present in transcription buffer but not present in TAE Mg^{2+} buffer. One possibility is that single-stranded overhangs may be required to enable proper nanotube growth in the presence of the spermidine in the transcription buffer. Spermidine is a polyamine which would primarily exist as a trivalent cation in transcription buffer and can stabilize non-canonical nucleic acid structures (1). Additionally, spermidine is a known DNA-condensing agent (2) and could promote tile or nanotube aggregation during annealing. To test whether spermidine was specifically causing issues with nanotube assembly we prepared an RNAPol transcription buffer without spermidine and annealed nanotubes with and without a single-stranded overhang domain in this buffer. We found that the var1_7 and var3_7 tiles variants without the single-stranded overhang assembled into nanotubes in transcription buffer when spermidine was not present (Supplementary Figure S1A and B). We also observed that large tile aggregates form when tile variants without the single-stranded overhang were annealed in transcription buffer with spermidine present (Supplementary Figure S1C). The single-stranded overhang domain which should point outward from the nanotubes into the surrounding solution (3) may help prevent this aggregation, allowing longer nanotubes to form in the transcription buffer where spermidine is present.

4 Denatured T7 RNAP nanotube stability experiments

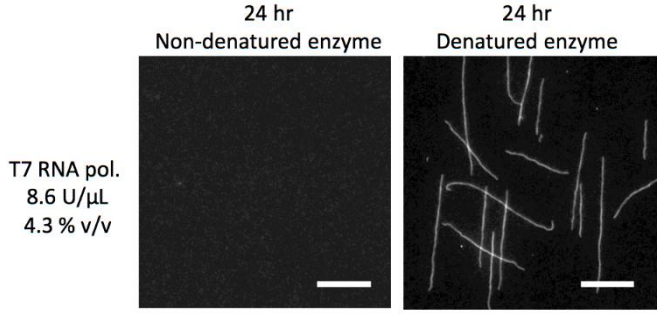

Supplementary Figure S2*:* Fluorescence micrographs of var3_7 nanotubes 24 hours after incubation with either active or heat denatured T7 RNAP. Experiments were conducted as described in *Measurement of nanotube stability* in the Methods of the main text. Concentration of DNA tiles: 1 µM. RNAP was denatured at 65°C for 30 minutes and then added to the nanotube mixture at the same volume as the sample with active polymerase. Scale bars: 10 µm.

5 SP6 RNAP nanotube stability assays

Supplementary Table S1: Name, product number, stock unit concentration, and unit definition of each of the RNA polymerases used in the nanotube stability assays.

Enzyme	Stock Units	Units Definition / Buffer conditions
T7 RNAP (Cellscript C-T7300K)	200 U/µL	One unit of RNA polymerase catalyzes the incorporation of 1 nmol of ribonucleoside triphosphate into RNA in 1 hour at 37°C under standard assay conditions using a DNA template with the appropriate T7 promoter. Storage buffer: 50% glycerol containing 50 mM Tris-HCl (pH 7.5), 0.1 M NaCl, 1.0 mM DTT, 0.1 mM EDTA, and 0.1% Triton® X-100.
SP6 RNAP (ThermoFisher EP0133)	100 U/µL	One unit of the enzyme incorporates 1 nmol of AMP into a polynucleotide fraction (adsorbed on DE-81) in 60 minutes at 37°C. Storage buffer: The enzyme is supplied in: 50 mM Tris-HCl (pH 8.0), 150 mM NaCl, 5 mM DTT, 0.1 mg/ml BSA, 0.03% (v/v) ELUGENT Detergent and 50% (v/v) glycerol.

The enzymes used in this study were purchased at different stock activity units (Supplementary Table S1). To compare nanotube stability when incubated with the different enzymes, all stability assays were conducted with the same enzyme activity units (8.6 U/µL).

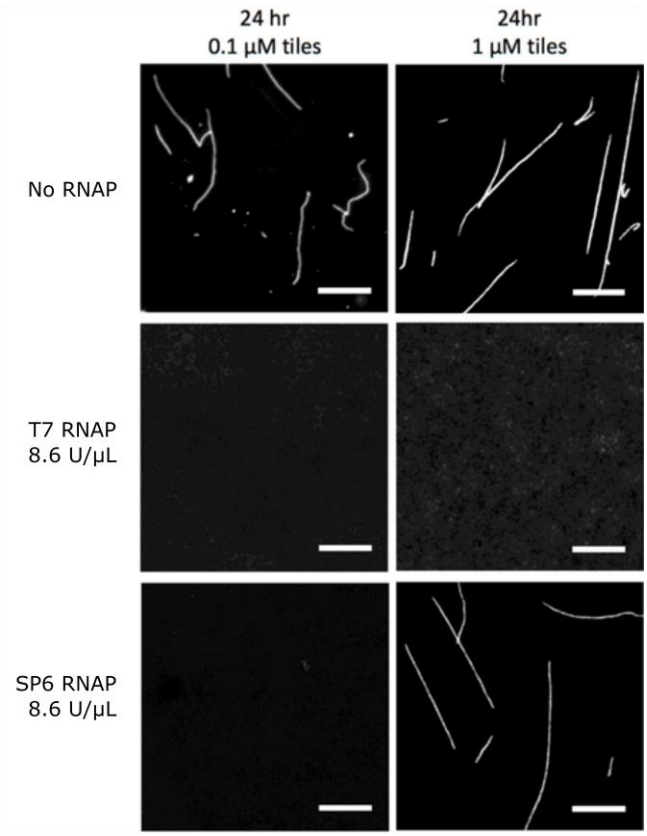

***Supplementary Figure S3**:* Fluorescence micrographs of var3_7 nanotubes incubated at 100 nM or 1 µM tile concentration with and without viral RNA polymerases at unit activity 8.6 U/µL. Experiments were conducted as described in *Measurement of nanotube stability* in the Methods of the main text. Scale bars: 10 µm.

6 Different T7 RNAP concentrations

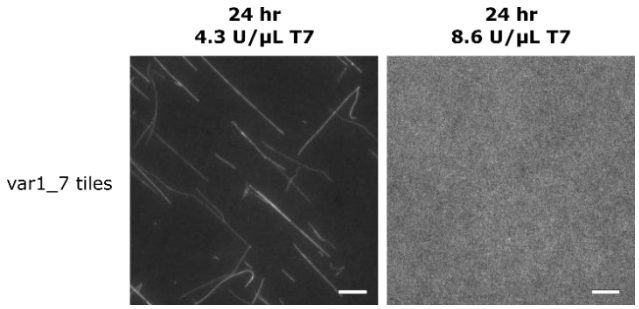

***Supplementary Figure S4**:* Fluorescence micrographs of var1_7 nanotubes 24 hours after incubation with T7 RNAP at 4.3 (left) or 8.6 U/µL (right). Experiments were conducted as described in *Measurement of nanotube stability* in the Methods of the main text. Concentration of DNA tiles: 1 µM. Scale bars: 10 µm.

7 DNA nanotubes with low overlap with viral RNAP promoter sequences

7.1 Design of DNA nanotube sequences with low overlap with viral RNAP promoter sequences

To test whether nanotube disassembly in the presence of viral RNAPs was caused by sequence-specific binding of the polymerases to sequences similar to viral RNAP promoters, we designed a new set of DNA tile sequences that had less sequence overlap with the promoter sequences of 3 common viral RNAPs (T7, T3, and SP6). We began this design process by collecting information about sequences that T7, T3, and SP6 RNAPs might bind to specifically. For each polymerase, we found a set of functional promoter sequences that were either obtained from the respective viral genomes (4) (in the case of SP6 and T3 RNAP), or were known to initiate transcription efficiently (5) (in the case of T7 RNAP). In each collection of promoter sequences, we assumed that the enzyme recognized the conserved bases in the sequence collection, and that those that were partially conserved were proportionally less important for sequence-specific binding of the polymerase. To represent this data, we created sequence logos, which are produced by aligning a set of functional sequences and graphically stacking the letters representing the nucleotides on top of each other at each position along the sequence. The height of an individual base in a stack is proportional to its frequency at that position in the sequence alignment and the total height of a stack represents the information content of the sequence at that position measured in bits (5) (Supplementary Figure S5A).

To avoid tile sequences that contained patterns of bases matching the conserved bases represented in the sequence logo data for each enzyme, we created a scoring function that penalizes sequences to an extent proportional to their overlap with all possible combinations of the conserved bases in the promoter sequences. We then generated a large library of potential designs and found a design with minimal overlap using the DNA Design Toolbox (http://www.dna.caltech.edu/DNAdesign).

To score a design, we used a 126 base pair sequence that repeats along a nanotube defined by a given set of tile sequences (Supplementary Figure S5B). We measured all possible ways a polymerase might bind to a promoter-like sequence within this sequence repeat by identifying all subsequences of the same length as the polymerase promoter sequence. For example, for T7 RNAP, the length of the promoter sequence we used was 23 nucleotides, so we separated a design into the 208 different 23-base subsequences it contained (accounting for the 5' to 3' sequences on both strands of the 126 base pair repeat region). For each subsequence the penalty for overlap with a library of promoter sequences for a specific viral RNAP was the sum over the total bases in this viral RNAP promoter:

$$subsequence\ score = \sum_{base=i}^{L} IC(i) * frequency(base(i))$$

where IC is the information content at a given position in the sequence logo data, frequency(base(i)) is the frequency at which the i^{th} base in the subsequence is found at the i^{th} position in the sequence logo, and L is the number of bases in the sequence logo data for a given polymerase (23 for T7 RNAP).

The scores for each subsequence along the repeating unit were summed to produce the following total design score for a given polymerase:

$$total\ polymerase\ design\ score = \sum_{subsequence=i}^{N} subsequence\ score(i)$$

where N is the total number of subsequences (*i.e.* 208). To create sequences that avoided overlap with the promoter sequences of the 3 selected viral RNAPs, we summed these total design scores to obtain a final score for each potential tile sequence as shown below:

$$final\ score = [total\ T7\ design\ score] + [total\ T3\ design\ score] + [total\ SP6\ design\ score]$$

This score was then added to the existing scoring function in the DNA Design Toolbox to evaluate a sequence. The DNA Design Toolbox uses Monte Carlo optimization to minimize the expected number of bases that are incorrectly paired or unpaired at equilibrium for a tile design based on predictions from the standard model of DNA secondary structure thermodynamics. The code used for this optimization, which describes how different sequences were scored, is available upon request. This total objective function was minimized to produce a new tile design, the var2_7 tiles.

To verify that this sequence design process reduced the number of potential promoter-like binding sites for viral RNAPs along the nanotube, we compared the highest subsequence score (and thus the greatest promoter overlap) in the var1_7 tiles with the highest subsequence score (and thus the greatest potential promoter overlap) in the designed var2_7 tiles for T7 RNAP. We found that the var2_7 tiles had a lower maximum subsequence score compared to the var1_7 tiles suggesting that the design process yield nanotubes that would be less likely to promote specific binding of T7 RNAP (Supplementary Figure S5C).

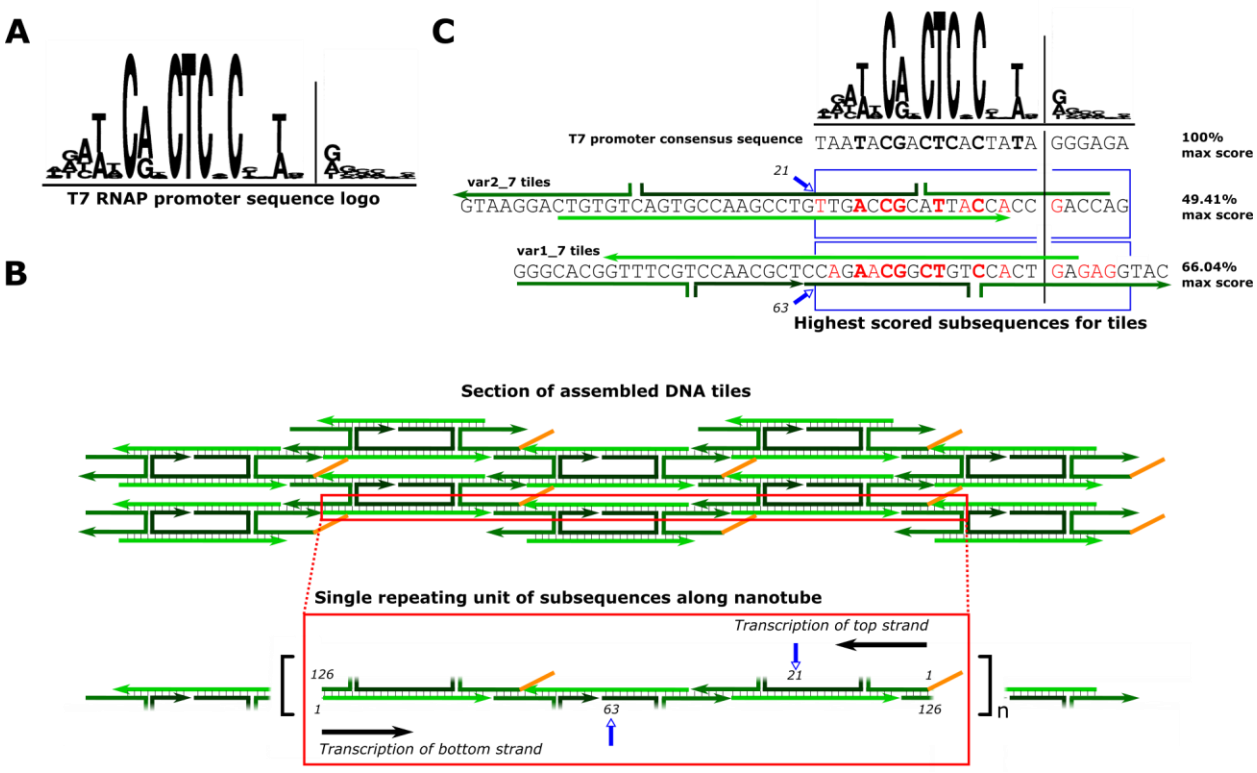

Supplementary Figure S5: Design of tile sequences with low overlap with viral RNAP promoter sequences. **A)** Sequence logo for functional mutant T7 RNAP promoters created from 53 mutant sequences (5). This data and analogous sequence logo data for T3 and SP6 RNAPs were used to minimize DNA tile sequence overlap with viral RNAP promoter sequences. The vertical line in the sequence logo is just to the left of the +1 position of transcription. **B)** Schematic of a single repeating sequence along the DNA nanotubes that was used for scoring tile sequences against the viral RNAP promoter sequence logo data. Transcription along the top and/or bottom strand is possible. Brackets indicate that this unit is repeated along the length of the DNA nanotube. The numbers indicate the 1st (5′ end) and 126th (3′ end) base position along each of the top and bottom strands. Blue arrows indicate the locations along the repeat of the subsequences that yielded the max score for the var1_7 tiles with respect to the T7 RNAP promoter sequence (bottom strand at position 63) and the var2_7 tiles (top strand at position 21). **C)** Schematic showing the subsequences of the var1_7 and var2_7 tiles that had the highest overlap scores with the T7 RNAP promoter sequences each aligned with the sequence logo data for T7 RNAP along with the score for each sequence as a percentage of the maximum possible overlap score (the maximum possible score is obtained by scoring a subsequence that is the most frequent base at each position of the sequence logo). The bolded bases in the consensus sequence shown below the logo are those corresponding to positions that contain only 1 or 2 bases in the sequence logo. The blue box surrounds the subsequences that are aligned with the consensus sequence above to show where the subsequences start and end. The vertical black line is just to the left of the +1 position of transcription in the consensus sequence. Bases in the subsequences that are contained in the consensus sequence are shown in red. Based in red and in bold are bases that match the consensus sequence at positions that only contain 1 or 2 bases in the sequence logo. Blue arrows show the position along the nanotube sequence repeat unit where the consensus sequence match starts as in B.

7.2 Stability of DNA nanotube with sequences that have low overlap with viral RNAP promoter sequences

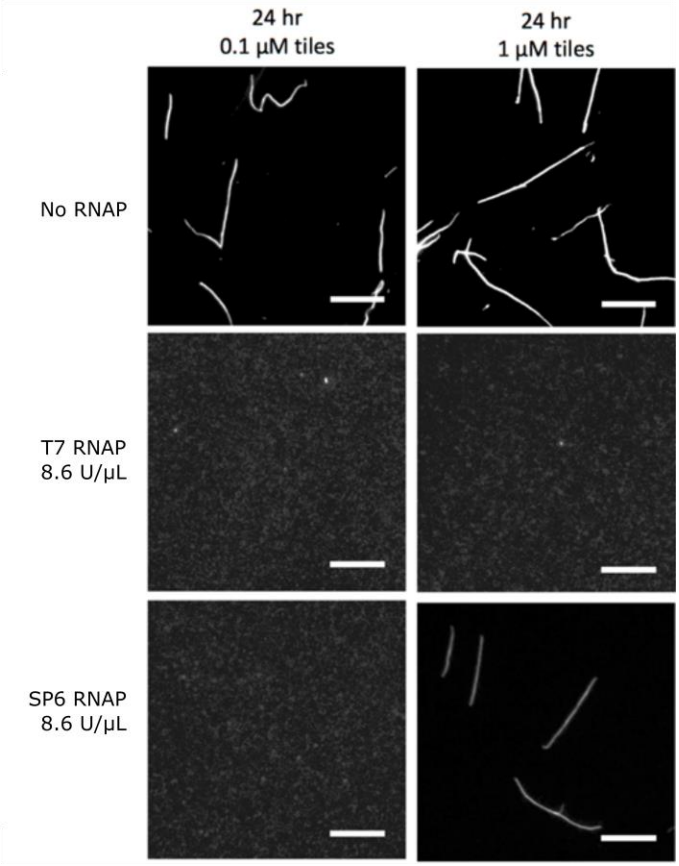

Supplementary Figure S6: Fluorescence micrographs of the var2_7 nanotubes incubated at either 100 nM or 1 µM tile concentration with and without T7 RNAP or SP6 RNAP in transcription conditions. Experiments were conducted as described in *Measurement of nanotube stability* in the Methods of the main text. Scale bars: 10 µm.

8 Stability of nanotubes variants with different sticky end sequences and lengths in the presence of T7 RNAP

8.1 Sticky end free energy calculations

To estimate the free energies of hybridization of the sticky end sequences in Figure 2 of the main text and Supplementary Figure S8, we used NUPACK (7) with a temperature of 37^{o}C and default salt conditions (1.0 M Na^{+}, 0.0 M Mg^{2+}). We calculated the free energy of hybridization of a motif that included the sticky end sequences and an additional base on either side of the sticky end sequence as shown in Figure 2 and Supplementary Figure S8. The flanking bases were included because, upon hybridization, the sticky ends will have the stacking interaction of the nucleotide across the nick in the DNA backbone (8). We assumed that this interaction was important for each set of sticky end pairs. While this interaction may be weaker for the sticky ends adjacent to the single-stranded overhang domain, this weaker interaction existed for all variants so ignoring it should not change predictions about which sticky ends are stronger or weaker than others.

8.2 Fluorescence micrographs of 7bp sticky end tile variants incubated with T7 RNAP

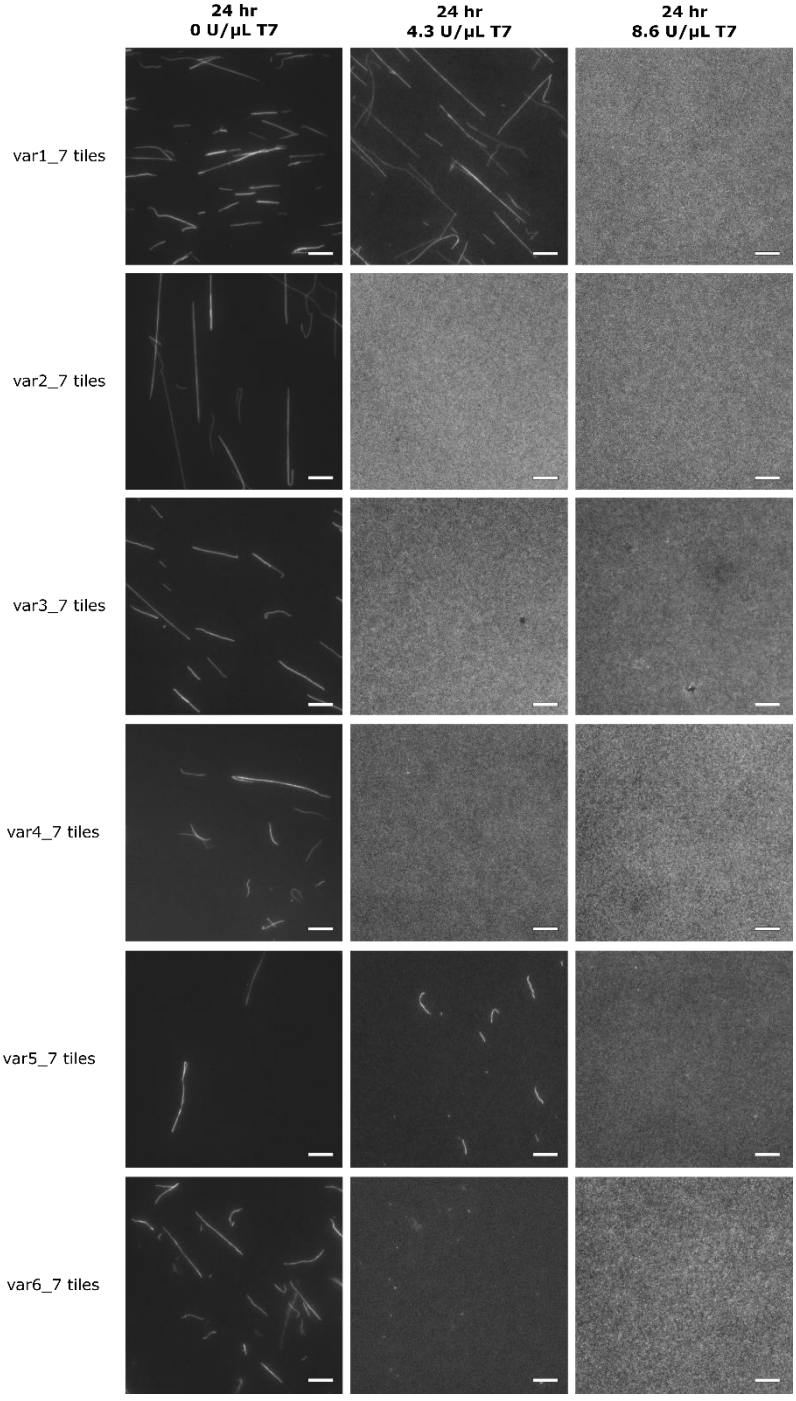

Supplementary Figure S7: Fluorescence micrographs of 7bp sticky end nanotube variants incubated with the amounts of T7 RNAP shown. Results are summarized in Figure 2 of the main text. Experiments were conducted as described in *Measurement of nanotube stability* in the Methods of the main text. Concentration of DNA tiles: 1 µM. Scale bars: 10 µm.

8.3 Design of 6bp sticky end and 8bp sticky end tile variants

To test whether sticky end length affected the stability of DNA nanotubes in the presence of viral RNA polymerases, we created a family of tiles with sticky ends of different lengths. Tiles in the first set have the same tile sequences as the var1_7 tiles but with sticky ends shortened or extended by 1 base (var1_6 or var1_8, respectively). Similarly, tiles in the second set have the same tile sequences as the var3_7 tiles but with sticky ends shortened or extended by 1 base (var3_6 or var3_8, respectively). Changes to the lengths of other strands in the tiles was done to maintain 21 bases between the inter-tile double crossover motifs (3).

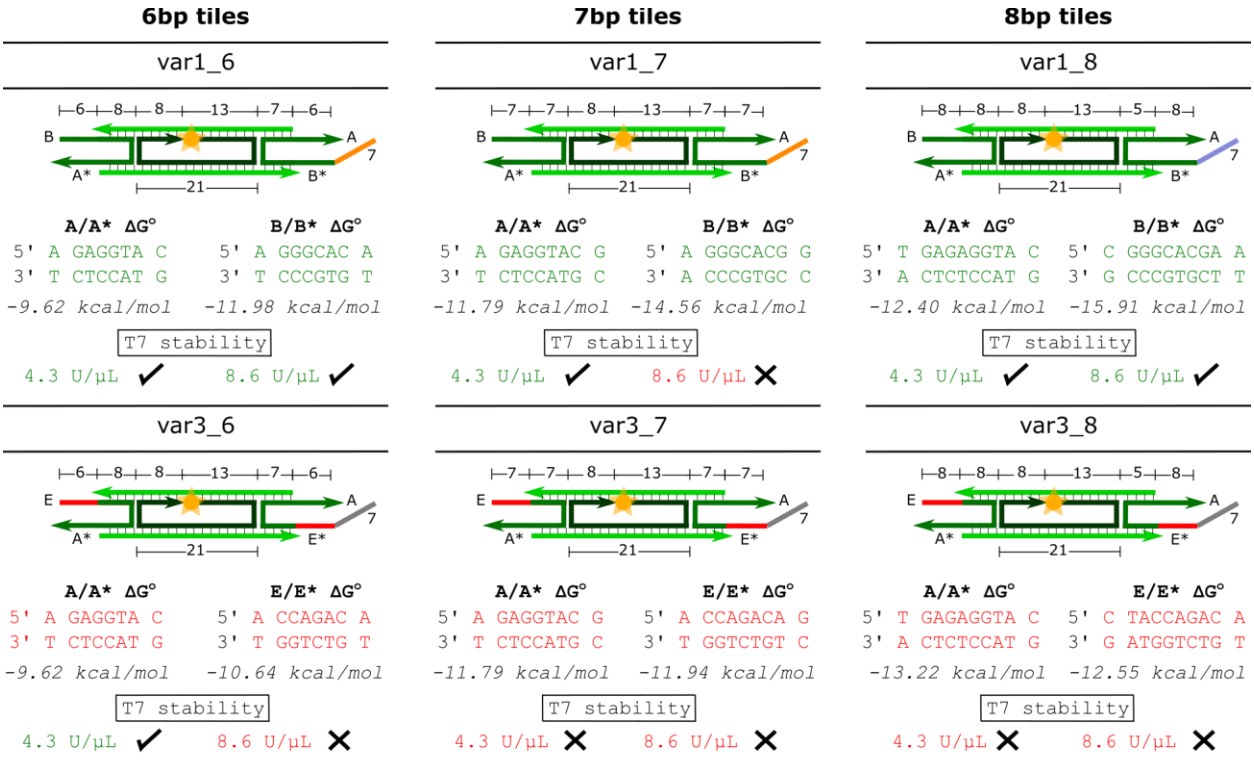

Supplementary Figure S8: The sticky end sequences, estimated sticky end energies, and the stability in the presence of T7 RNAP of nanotubes with 6, 7, and 8 base pair sticky ends. The domains of variants whose sequences are different from the sequences of the respective domains in var1_7 are shown in different colors than the domains in var1_7 (SI Section 1 for sequences). Numbers next to domains indicate domain length in number of bases. Free energies were estimated for comparison using NUPACK (7) (SI Section 8.1). Nanotubes were deemed stable (check) at the enzyme unit concentration listed if nanotubes at 1 µM tile concentration were present after 24 hours of incubation with T7 RNAP and were deemed unstable (X) if no nanotubes were present after this incubation. Fluorescence micrographs of the samples are shown in Supplementary Figure S9.

8.4 Fluorescence micrographs of 6 and 8bp sticky end tile variants incubated with T7 RNAP

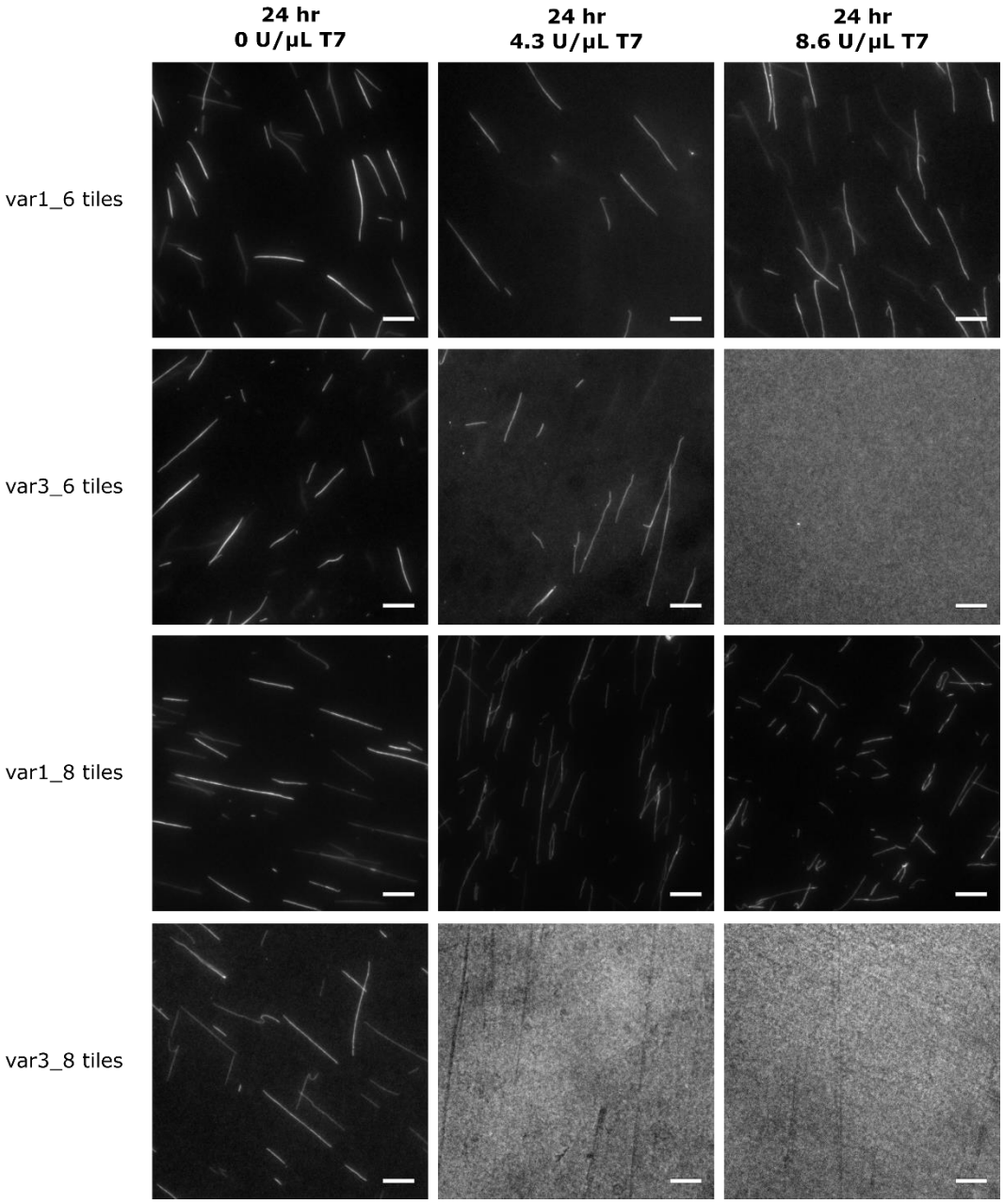

Supplementary Figure S9: Fluorescence micrographs of nanotube with 6 and 8bp sticky ends incubated with the amounts of T7 RNAP shown. The results here are summarized in Supplementary Figure S8. Experiments were conducted as described in *Measurement of nanotube stability* the Methods of the main text. Concentration of DNA tiles: 1 µM. Scale bars: 10 µm.

9 Influence of Mg^{2+} concentration on nanotubes with T7 RNAP

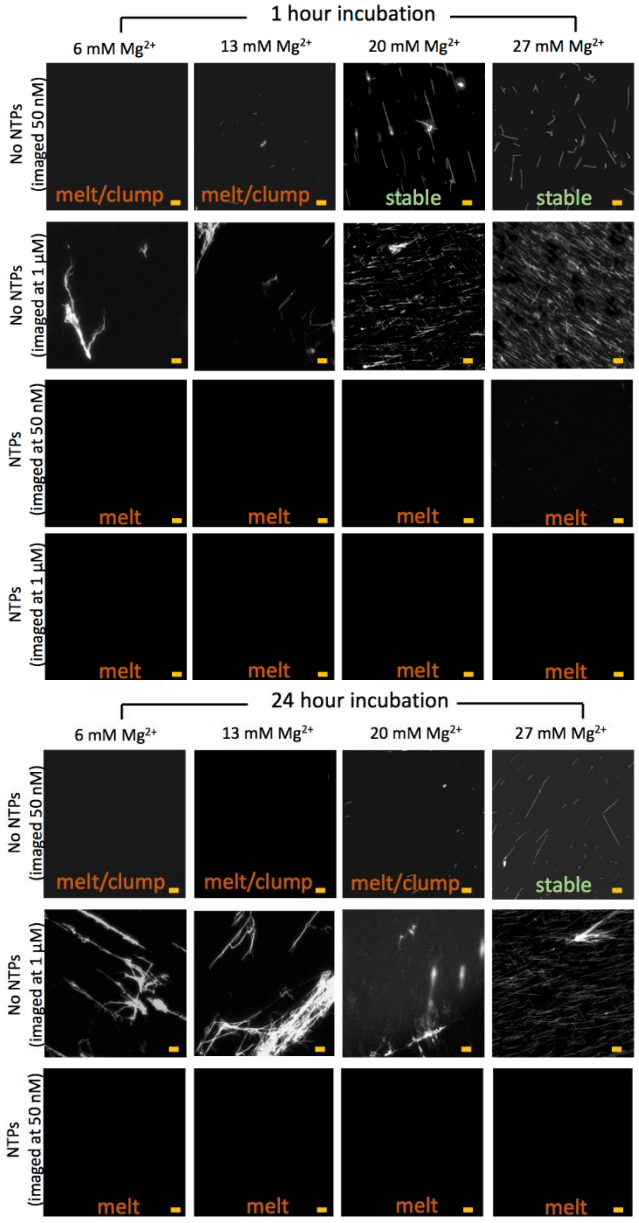

***Supplementary Figure S10*:** Fluorescence micrographs of var3_7 nanotubes incubated in the presence of T7 RNAP with and without NTPs and at different total Mg^{2+} concentrations. Samples imaged after 1 hour or 24 hours with T7 RNAP (same imaging procedure as in the Methods of the main text except samples were imaged without dilution when imaged as indicated at 1 µM). Experiments were conducted as described in *Measurement of nanotube stability* in the Methods of the main text. Concentration of DNA tiles: 1 µM and concentration of T7 RNAP: 8.6 U/µL. At low Mg^{2+} concentration in absence of NTPs, nanotubes appear to clump together. The presence of T7 RNAP and NTPs results in complete nanotube disassembly at all Mg^{2+} concentrations after 1 hour. Scale bars: 10 µm. T7 RNAP has been shown to aggregate at low ionic strengths (9) so one possibility is that low Mg^{2+} concentrations causes T7 RNAP molecules to aggregate while bound to DNA nanotubes, resulting in the observed nanotube clumping.

10 Nanotubes incubated with T7 RNAP and either GTP, CTP, or UTP

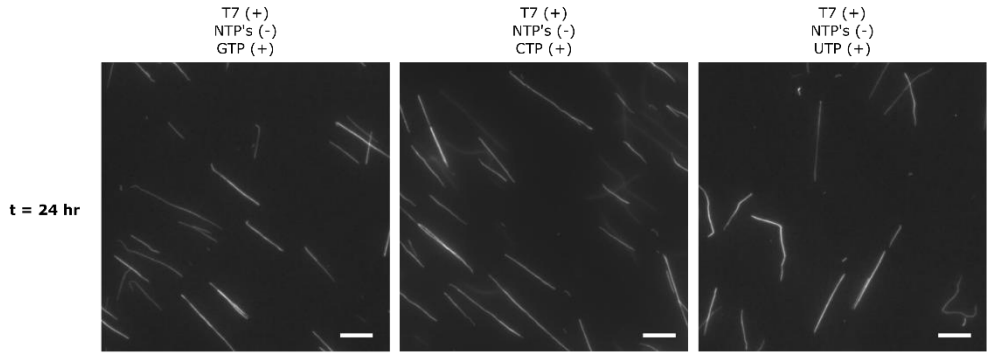

Supplementary Figure S11: Fluorescence micrographs of var1_7 nanotubes incubated with only the NTP types shown and T7 RNAP for 24 hours. Experiments were conducted as described in *Measurement of nanotube stability* of the Methods of the main text. Concentration of individual NTPs: 20 mM in each experiment, concentration of DNA tiles: 1 µM, and concentration of T7 RNAP: 8.6 U/µL. Scale bars: 10 µm.

The presence of T7 RNAP and GTP alone has been shown to allow the enzyme to undergo transcription initiation and engage in abortive cycling where short (<10 nucleotides) transcripts are repeatedly produced. However, the absence of the other NTP species prevents the enzyme from entering a processive elongation state (10, 11). Transcription initiation melts a segment of DNA so if transcription initiation were responsible for nanotube disassembly, the incubation of nanotubes with T7 RNAP and GTP should result in nanotube disassembly. However, no difference was observed in the stability of nanotubes incubated with GTP and nanotubes incubated with other single NTP types.

11 T7 RNAP, nanotubes, or NTPs are required for the production of RNA transcripts

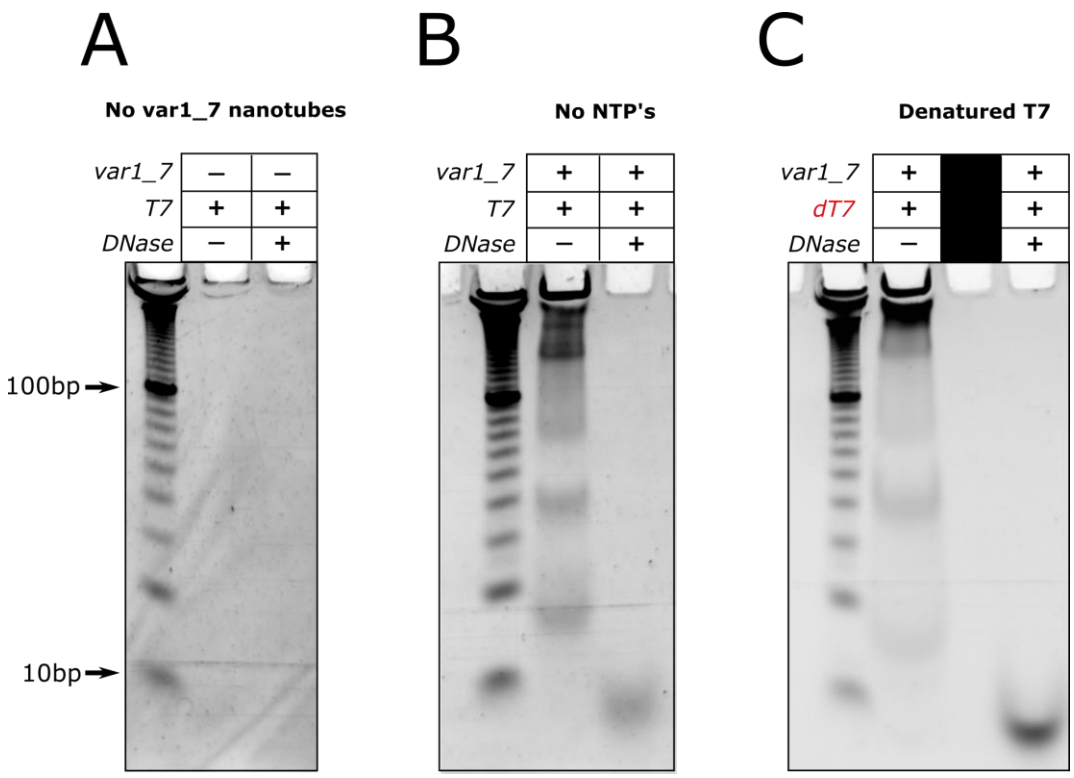

Supplementary Figure S12: RNA is not produced when var1_7 nanotubes, NTPs, or active T7 RNAP are absent during the initial 20 hour T7 RNAP incubation step. These experiments were performed as described in *Characterization of RNA transcript* in the Methods of the main text except that the indicated components were not present or changed. **(A-C)** Non-denaturing PAGE results. T7 RNAP (T7), DNase I (DNase), and nanotubes (NT) are in each sample as shown. **A)** No gel products are observed if DNA nanotubes are absent during T7 RNAP incubation in transcription conditions. **B)** No RNA products are observed when nanotube are incubated with T7 RNAP in transcription conditions without NTPs. Because T7 RNAP does not require NTPs to bind DNA templates (10, 12), the lack of products in lane 3 indicates that DNase I completely digests nanotube DNA even in the presence of T7 RNAP. **C)** No RNA products are observed when nanotubes are incubated with denatured T7 RNAP (8.6 U/µL) in transcription conditions. T7 RNAP was denatured at 65°C for 30 minutes. Bands at the bottom of the gels (migrating more slowly than 10bp DNA migrates) for the samples incubated with DNase I are likely short oligonucleotides that remain after DNase I digestion.

12 RNA transcripts bind to DNA strands from their respective transcription templates but not to other DNA

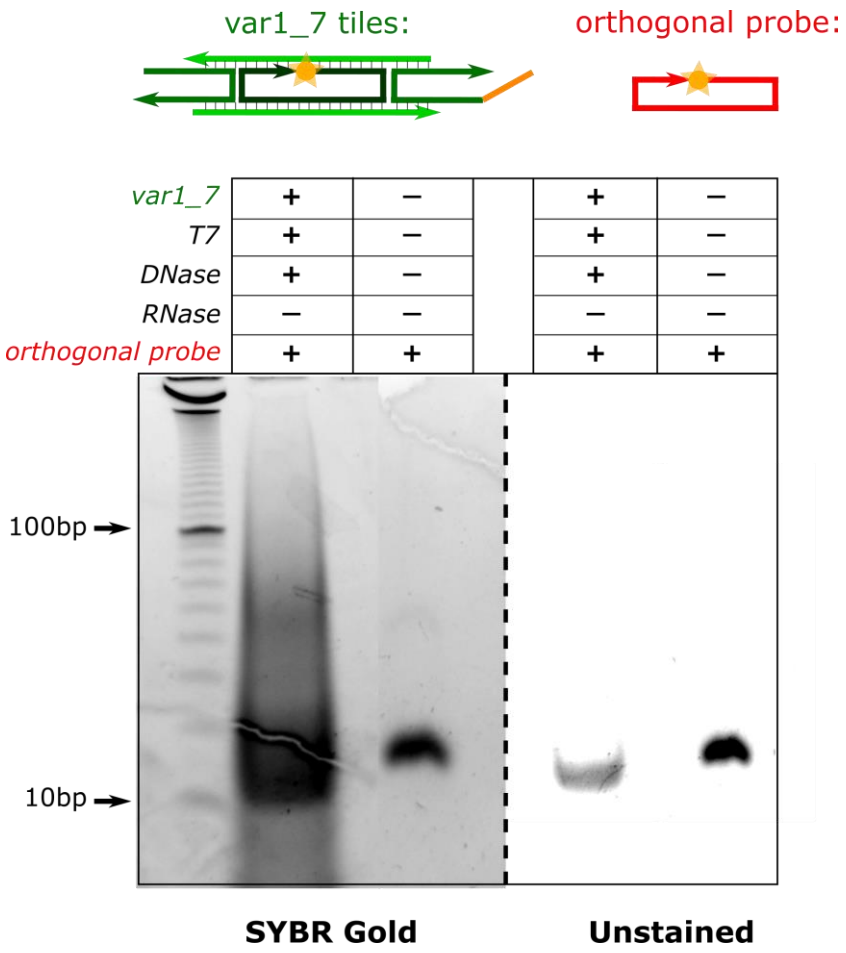

Supplementary Figure S13: An orthogonal sequence probe with no sequence overlap with the var1_7 tiles does not bind to the transcript produced during incubation of var1_7 nanotubes with T7 RNAP. Nanotubes (NT), orthogonal probe (ortho. probe), T7 RNAP (T7), DNase I (DNase), and RNase A (RNase) are present in samples as shown. These experiments were conducted as described in *Detecting tile-specific sequences in RNA with fluorescent DNA probes* in the Methods of the main text except that samples were incubated with DNase I for just 2 hours. Schematics of the nanotube tile variant used during the T7 RNAP incubation to produce RNA and the orthogonal fluorescence probe (SI Section 1.2 for sequence) are shown at the top of the figure.

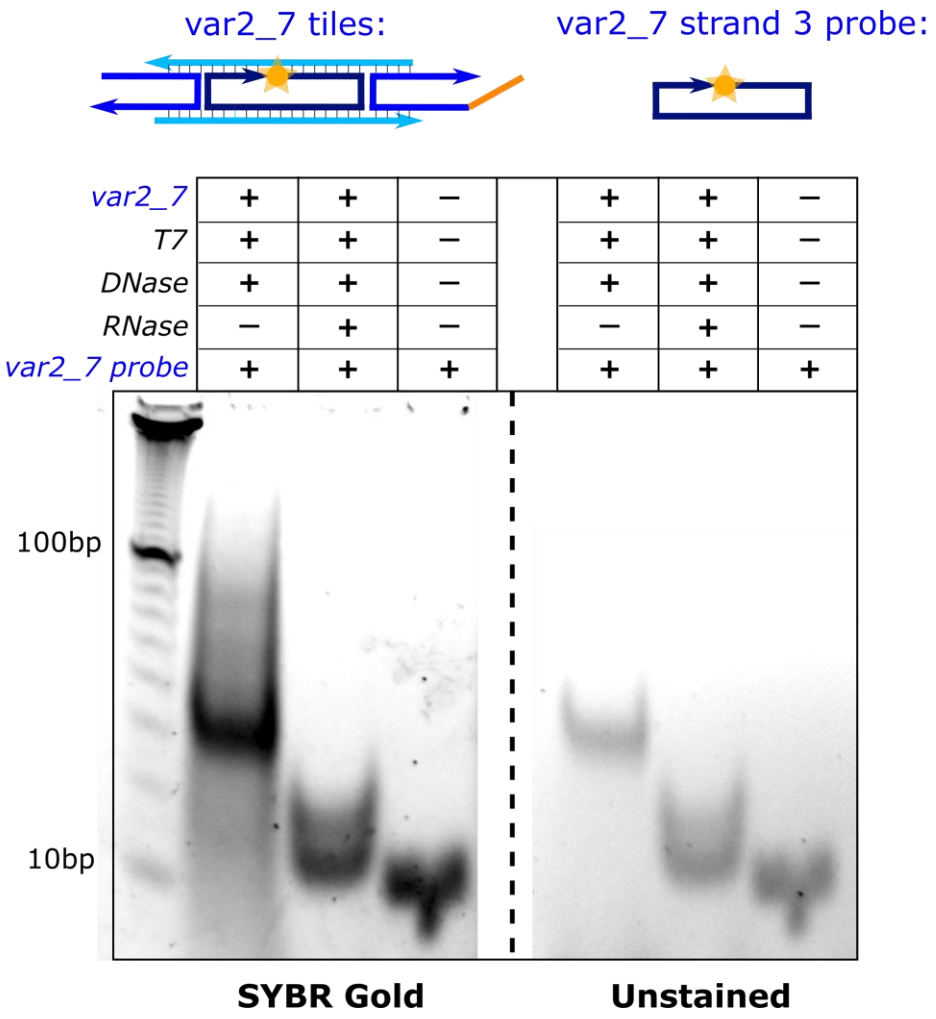

Supplementary Figure S14: var2_7 nanotubes incubated with T7 RNAP in transcription conditions produce RNA that binds the var2_7 probe (SI section 1.2 for sequence). Nanotubes (NT), var2_7 probe, T7 RNAP (T7), DNase I (DNase), and RNase A (RNase) are present in samples as shown. These experiments were conducted as described in *Detecting tile-specific sequences in RNA with fluorescent DNA probes* in the Methods of the main text. Schematics of the nanotube tile variant used during the T7 RNAP incubation to produce RNA and the var2_7 fluorescence probe (SI Section 1 for sequences) are shown at the top of the figure.

13 DNA nanotube stability in the presence of both T7 RNAP and RNase A

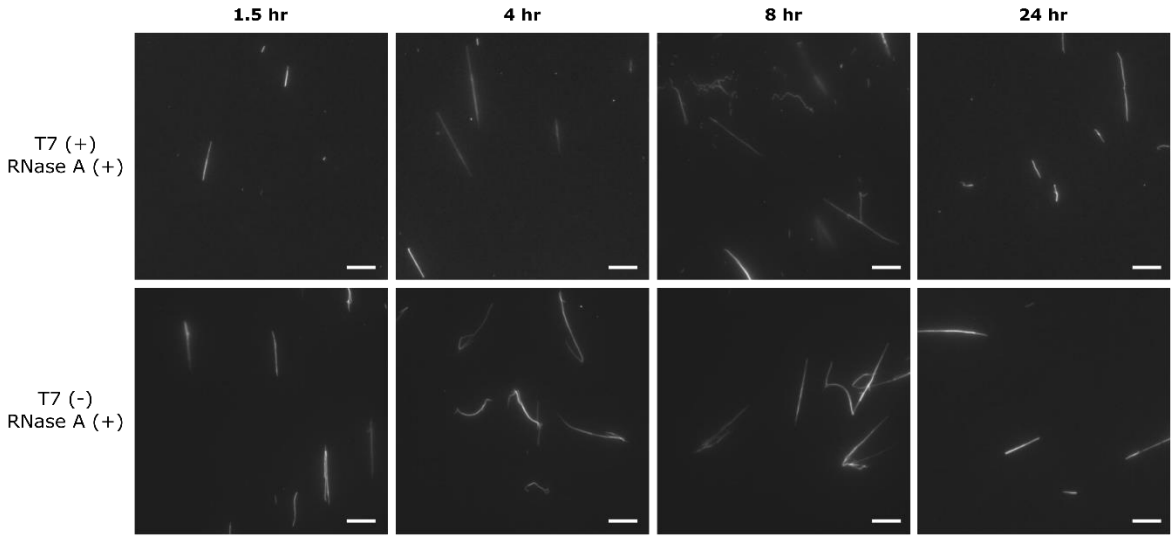

Supplementary Figure S15: RNase A prevents var1_7 DNA nanotube disassembly in the presence of T7 RNAP. Fluorescence micrographs of nanotubes incubated for different times with RNase A (0.06 U/μL) and with or without T7 RNAP (8.6 U/μL). Experiments were conducted as described in *Measurement of nanotube stability* in the Methods of the main text. Concentration of DNA tiles: 1 μM. Scale bars: 10 μm. The presence of nanotubes at each of the time points suggests that nanotubes did not disassemble at the beginning of the experiment due to a high transcription rate and then reform as NTPs were exhausted and the RNA was digested by RNase A.

14 Nanotube stability with RNA transcripts produced from T7 RNAP incubation

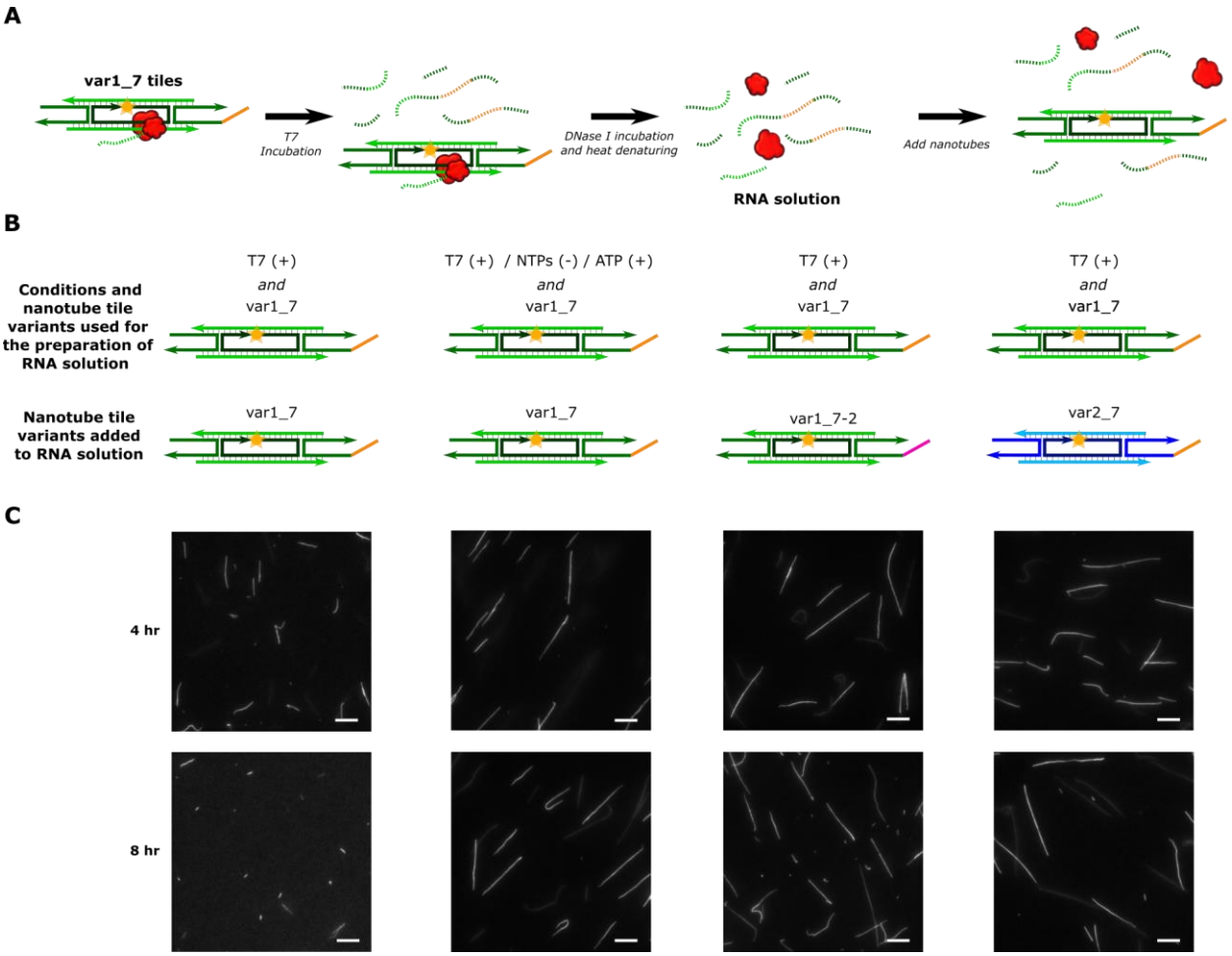

Supplementary Figure S16: RNA produced during the incubation of DNA nanotubes and T7 RNAP in transcription conditions (Methods of the main text) can disassemble DNA nanotubes. **A)** Schematic showing the steps of the RNA solution preparation process. A protocol similar to the one detailed in *Detecting tile specific sequences in RNA with fluorescent DNA probes* in the Methods of the main text was followed; however samples were only treated with DNase I. After heat denaturing DNase I, no annealing step was performed and intact nanotubes were added to the RNA solution (to a final concentration of 795 nM) at 37°C and incubated for 8 hours (see SI Section 2 for PCR protocol details). **B)** The reaction conditions and the nanotube tile variants used to prepare an RNA solution in each set of experiments (top row) and the nanotube tile variant added to the RNA solution after DNase I DNA degradation and denaturation (bottom row). **C)** Fluorescence micrographs of the nanotubes in each of the experiments in B after different incubation times with the RNA solution. Nanotube imaging was conducted as described in *Measurement of nanotube stability* in the Methods of the main text. Scale bars: 10 μm.

15 Confirmation of FAM fluorescence change system

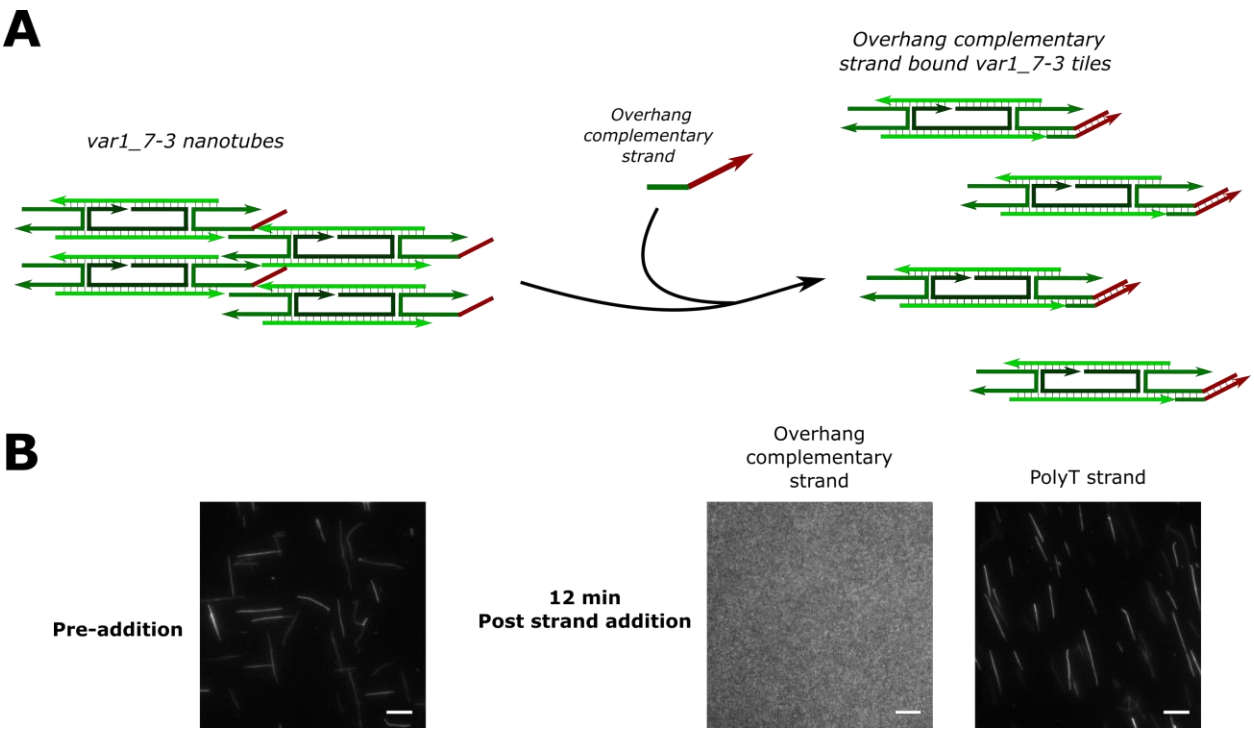

Supplementary Figure S17: var1_7-3 nanotubes can be disassembled in the presence of a DNA overhang complementary strand: a DNA strand consisting of the complement of the single-stranded overhang region of the tiles and the complement of the adjacent sticky end (sequence in SI Section 1.3). **A)** Schematic of the hypothesized reaction between the complementary DNA strand and the tiles or nanotubes. The overhang complementary strand should bind to the single-stranded overhang domain on the nanotubes and disrupt the sticky end hybridization interaction between tiles or prevent sticky end hybridization of free tiles. Disruption of tile sticky end hybridization should cause DNA nanotubes to disassemble. **B)** Fluorescence micrographs of var1_7-3 nanotubes after the addition of either the DNA overhang complementary strand or a 20 base poly-T strand as a control. The overhang complementary strand or the poly-T strand were added to their respective samples to final concentrations of 2 µM. Addition of the overhang complementary strand caused the nanotubes to disassemble. Nanotube imaging and reactions were conducted as described in *Measurement of nanotube stability* in the Methods of the main text. Scale bars: 10 µm. var1_7-3 nanotubes were prepared as described in *Detecting interactions between the RNA transcript and the DNA nanotubes* in the Methods of the main text with 25% of strand 2 of the tiles modified with a 5' FAM molecule. Reactions were conducted at 37°C in NEB RNApol Reaction Buffer with a final concentration of 7.5 mM for each NTP, 30 mM of $MgCl_2$, biotinylated BSA at 0.1 mg/mL, and nanotubes at 1 µM tile concentration. The images were taken using samples collected from the experiment shown in Supplementary Figure S18.

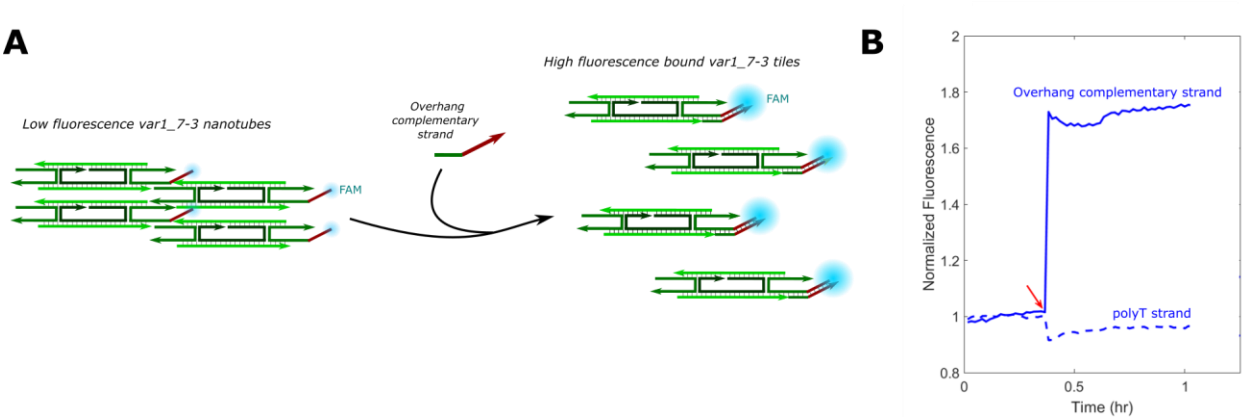

Supplementary Figure S18: The intensity of fluorescence from a FAM molecule at the 5' end of the single-stranded overhang domain of strand 2 of the tiles changes when DNA hybridizes to the overhang domain. **A)** Schematic of the postulated reaction and change in fluorescence. The overhang complementary strand should bind to the single-stranded overhang domain on the nanotubes and displace the adjacent sticky end. This hybridization should change the fluorescence emitted by the FAM molecule and also cause DNA nanotubes to disassemble as shown in Supplementary Figure S17. **B)** Fluorescence intensity of the nanotube samples over time before and after adding either the overhang complementary strand or a 20 nucleotide poly-T strand (each to a final concentration of 2 µM). Fluorescence data was normalized by dividing by the fluorescence intensity of the sample at t = 0. Reactions were run in a quantitative PCR machine as described in *Detecting interactions between the RNA transcript and the DNA nanotubes* in the Methods of the main text. FAM-modified var1_7-3 nanotubes were prepared as described in *Detecting interactions between the RNA transcript and the DNA nanotubes* in the Methods of the main text. To keep the fluorescence signal from saturating the detector, only 25% of strand 2 of the tiles contained the 5' FAM molecule. Reactions were conducted at 37°C in NEB RNApol Reaction Buffer with a final concentration of 7.5 mM for each NTP, 30 mM of $MgCl_2$, biotinylated BSA at 0.1 mg/mL, and nanotubes at 1 µM tile concentration. The fluorescence micrographs shown in Supplementary Figure S17 were taken from the samples presented in B.

16 Stability of nanotubes without a single-stranded overhang domain

16.1 Nanotubes without a single-stranded overhang are stable with T7 RNAP

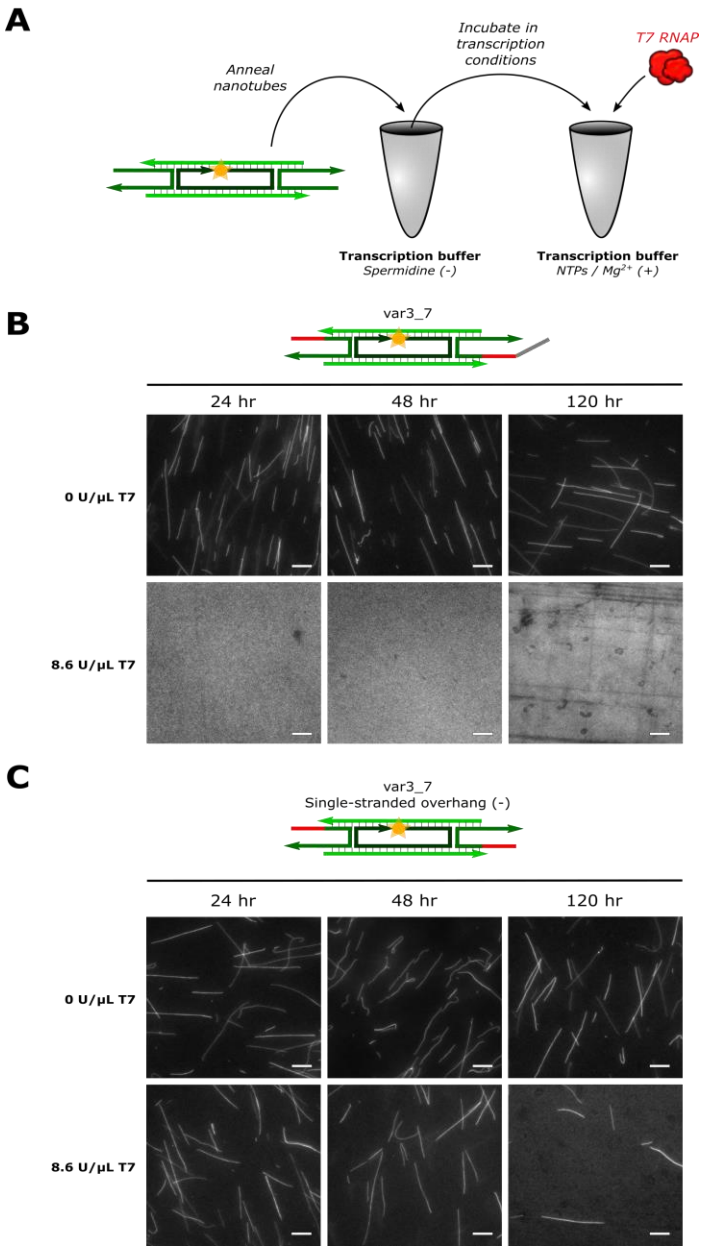

Supplementary Figure S19: Nanotubes without a single-stranded overhang are stable for at least 48 hours in the presence of T7 RNAP in transcription conditions. **A)** Schematic of the experimental procedure. Since nanotubes without a single-stranded overhang do not assemble in NEB RNAPol transcription buffer (Supplementary Figure S1), tile variants for this experiment were first annealed in RNAPol transcription buffer prepared without spermidine. The assembled nanotubes were then incubated with T7 RNAP in transcription conditions (with NEB RNAPol transcription buffer which contains spermidine) and imaged after incubation. **B)** and **C)** Fluorescence micrographs of the var3_7 nanotubes **B)** with and **C)** without a single-stranded overhang domain incubated in transcription conditions with the amounts of T7 RNAP shown. For the variant without the single-stranded overhang, there appeared to be fewer nanotubes per field of view after 120 hours, indicating that some slow disassembly may have occurred. Experiments were conducted as described in *Measurement of nanotube stability* the Methods of the main text. Concentration of DNA tiles: 1 µM. Scale bars: 10 µm.

16.2 Nanotubes with a double-stranded hairpin overhang domain are stable with T7 RNAP

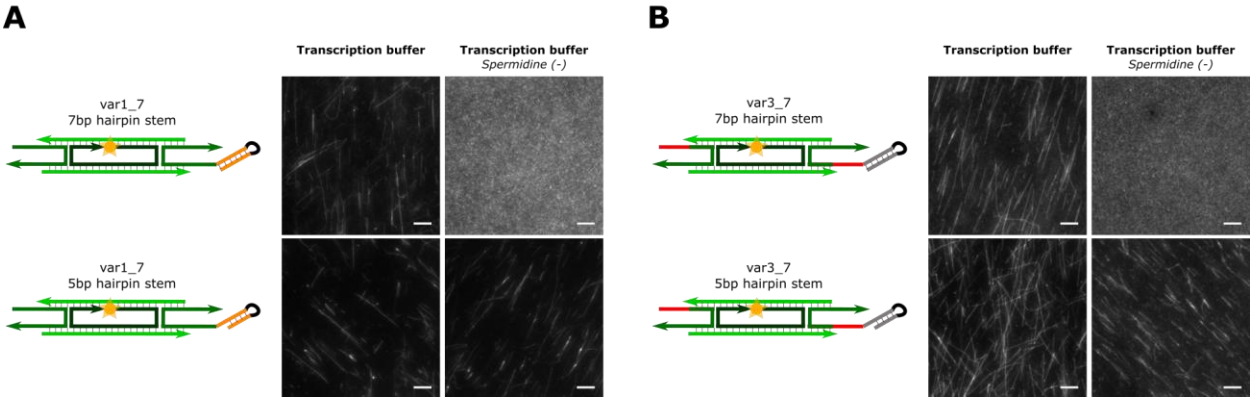

Supplementary Figure S20: Nanotubes with a double-stranded hairpin overhang assemble in transcription buffer. **A)** and **B)** Fluorescence micrographs of **A)** var1_7 nanotubes or **B)** var3_7 nanotubes with either a 7bp (top panel) or 5bp (bottom panel) hairpin stem on the double-stranded overhang annealed in transcription buffer or transcription buffer without spermidine. Nanotubes were annealed as described in *Measurement of nanotube stability* the Methods of the main text. Fluorescence micrographs were taken after diluting samples to a tile concentration of 250 nM. Scale bars: 10 µm. The variants with the 7bp hairpin stem have the entire single-stranded domain covered in double-stranded DNA and the variants with the 5bp hairpin stem have the two bases adjacent to the sticky end un-hybridized (sequences are available in Supplementary Section 1). Both tile variants with the 7bp hairpin stem do not assemble in transcription buffer without spermidine. In these variants the base of the hairpin stem is directly adjacent to the sticky end of the tile and perhaps steric or electrostatic interactions disrupt sticky end hybridization. The 7bp hairpin stem variants do assemble in transcription buffer (where spermidine is present). Spermidine may be able to mitigate issues with the assembly of the assembly of the 7bp hairpin stem tiles since spermidine can stabilize non-canonical DNA structures (1).

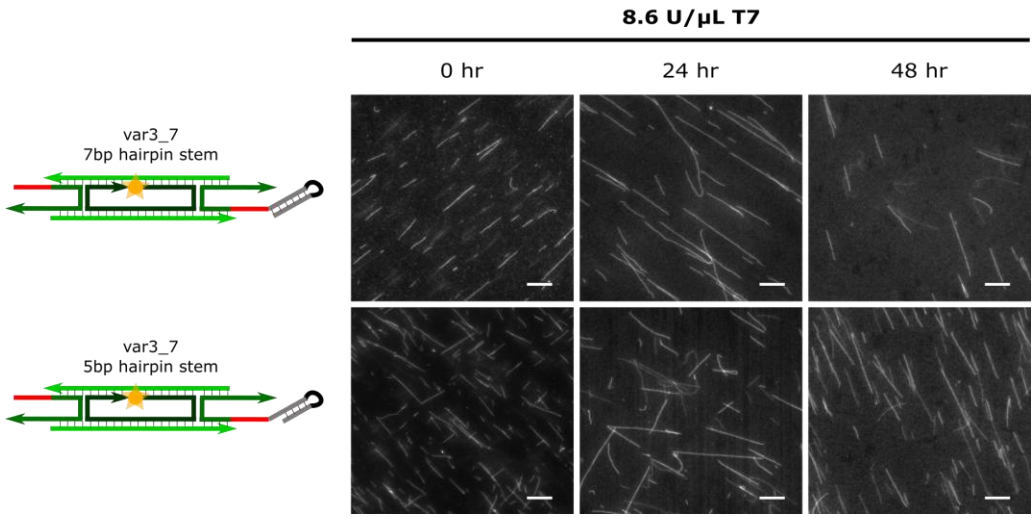

Supplementary Figure S21: Fluorescence micrographs of var3_7 nanotubes with either a 7bp (top panel) or 5bp (bottom panel) hairpin stem on the double-stranded overhang incubated in transcription conditions with T7 RNAP at the shown concentration. Concentration of DNA tiles: 1 µM. Scale bars: 10 µm.

References

1. Hou,M.-H., Lin,S.-B., Yuann,J.-M.P., Lin,W.-C., Wang,A.H.J. and Kan,L. (2001) Effects of polyamines on the thermal stability and formation kinetics of DNA duplexes with abnormal structure. *Nucleic Acids Res.*, **29**, 5121–5128.

2. Pardatscher,G., Bracha,D., Daube,S.S., Vonshak,O., Simmel,F.C. and Bar-Ziv,R.H. (2016) DNA condensation in one dimension. *Nat. Nanotechnol.*, **11**, 1076–1081.

3. Rothemund,P.W.K., Ekani-Nkodo,A., Papadakis,N., Kumar,A., Fygenson,D.K. and Winfree,E. (2004) Design and Characterization of Programmable DNA Nanotubes. *J. Am. Chem. Soc.*, **126**, 16344–16352.

4. Chen,Z. and Schneider,T.D. (2005) Information theory based T7-like promoter models: classification of bacteriophages and differential evolution of promoters and their polymerases. *Nucleic Acids Res.*, **33**, 6172–6187.

5. Schneider,T.D. and Stephens,R.M. (1990) Sequence logos: a new way to display consensus sequences. *Nucleic Acids Res.*, **18**, 6097–6100.

6. Schneider,T.D. and Stormo,G.D. (1989) Excess information at bacteriophage T7 genomic promoters detected by a random cloning technique. *Nucleic Acids Res.*, **17**, 659–674.

7. Zadeh,J.N., Steenberg,C.D., Bois,J.S., Wolfe,B.R., Pierce,M.B., Khan,A.R., Dirks,R.M. and Pierce,N.A. (2011) NUPACK: Analysis and design of nucleic acid systems. *J. Comput. Chem.*, **32**, 170–173.

8. SantaLucia,J. (1998) A unified view of polymer, dumbbell, and oligonucleotide DNA nearest-neighbor thermodynamics. *Proc. Natl. Acad. Sci. U. S. A.*, **95**, 1460–1465.

9. Maslak,M. and Martin,C.T. (1994) Effects of Solution Conditions on the Steady-State Kinetics of Initiation of Transcription by T7 RNA Polymerase. *Biochemistry*, **33**, 6918–6924.

10. Gunderson,S.I., Chapman,K.A. and Burgess,R.R. (1987) Interactions of T7 RNA polymerase with T7 late promoters measured by footprinting with methidiumpropyl-EDTA-iron(II). *Biochemistry*, **26**, 1539–1546.

11. Martin,C.T., Muller,D.K. and Coleman,J.E. (1988) Processivity in early stages of transcription by T7 RNA polymerase. *Biochemistry*, **27**, 3966–3974.

12. Bandwar,R.P. and Patel,S.S. (2002) The Energetics of Consensus Promoter Opening by T7 RNA Polymerase. *J. Mol. Biol.*, **324**, 63–72.